LETTER

https://doi.org/10.1038/s41586-019-0951-7

Wetland carbon storage controlled by millennial-scale variation in relative sea-level rise

Kerrylee Rogers[1]*, Jeffrey J. Kelleway[2], Neil Saintilan[2], J. Patrick Megonigal[3], Janine B. Adams[4], James R. Holmquist[3], Meng Lu[3,5], Lisa Schile-Beers[3], Atun Zawadzki[6], Debashish Mazumder[6] & Colin D. Woodroffe[1]

Coastal wetlands (mangrove, tidal marsh and seagrass) sustain the highest rates of carbon sequestration per unit area of all natural systems[1,2], primarily because of their comparatively high productivity and preservation of organic carbon within sedimentary substrates[3]. Climate change and associated relative sea-level rise (RSLR) have been proposed to increase the rate of organic-carbon burial in coastal wetlands in the first half of the twenty-first century[4], but these carbon–climate feedback effects have been modelled to diminish over time as wetlands are increasingly submerged and carbon stores become compromised by erosion[4,5]. Here we show that tidal marshes on coastlines that experienced rapid RSLR over the past few millennia (in the late Holocene, from about 4,200 years ago to the present) have on average 1.7 to 3.7 times higher soil carbon concentrations within 20 centimetres of the surface than those subject to a long period of sea-level stability. This disparity increases with depth, with soil carbon concentrations reduced by a factor of 4.9 to 9.1 at depths of 50 to 100 centimetres. We analyse the response of a wetland exposed to recent rapid RSLR following subsidence associated with pillar collapse in an underlying mine and demonstrate that the gain in carbon accumulation and elevation is proportional to the accommodation space (that is, the space available for mineral and organic material accumulation) created by RSLR. Our results suggest that coastal wetlands characteristic of tectonically stable coastlines have lower carbon storage owing to a lack of accommodation space and that carbon sequestration increases according to the vertical and lateral accommodation space[6] created by RSLR. Such wetlands will provide long-term mitigating feedback effects that are relevant to global climate–carbon modelling.

Broad biogeographic drivers, such as vegetation, climate, topography or water chemistry, are often emphasized as important global-scale controls on organic matter accumulation, decomposition and carbon stocks within tidal wetlands[7]. However, relative sea-level trends over the Holocene varied across the globe, principally on the basis of distance from maximal ice-sheet extent during the last glacial period, and have a profound influence on the contemporary character of coastal wetlands[8,9]. In Europe and North America, where studies of coastal wetland sea-level rise (SLR) impacts are concentrated, sea levels have been rising over the past few millennia at a decelerating rate up to the present (Fig. 1a, b). Tidal marshes in these locations, particularly when sediment supply is low–moderate, are often characterized by deep sediments that are highly organic[4,10,11], in contrast to coastal wetlands in locations where the sea level has been stable for the past few millenia[12], in spite of similarities in floristics[13].

We review published data, contribute new observations on soil carbon concentrations (%C) in tidal-marsh sediments and compare %C values over the active root zone (0–20 cm) and sub-surface depths (20–50 cm, 50–100 cm and >1 m) for 345 locations that vary in rates of SLR over the late Holocene (Supplementary Information). We find that variation in RSLR over past millennia is a primary control on carbon storage. Overall %C varies consistently between RSLR zones (areas spatially differentiated on the basis of consistent patterns of RSLR, fall or stability over the past 6,000 years) with concentrations in the upper 1 m significantly higher ($P < 0.001$) in zones subject to high rates of RSLR over the late Holocene (that is, zones I–II and II in Fig. 1) compared with zones subject to relative sea-level stability over the same period (that is, zones IV and V; Fig. 2, Extended Data Tables 1, 2). The upper metre of soil is the standard endorsed by the Intergovernmental Panel on Climate Change (IPCC) for tidal-wetland carbon-stock estimation[14], and in stable-sea-level zones it integrates processes over several thousand years[15,16]. Where data at depths exceeding 1 m are available, we find that this pattern of high storage in zones exhibiting RSLR over the past few millennia persisted (Fig. 2). Furthermore, the decline in %C with depth was greater in zones where sea level was relatively stable (that is, IV and V), yet remained relatively high in zones where rates of RSLR were high (Fig. 2, Extended Data Table 3; $P < 0.001$ for all pairwise comparisons). Trends were consistent with these findings in zones I and III, as well as in transitional regions, although relatively few data were available from these locations (Extended Data Fig. 1, Extended Data Table 3).

Models emphasizing biotic controls over coastal wetland elevation response to SLR have been largely derived from coasts with ongoing long-term SLR[11,17], where the vertical space available for mineral and organic material accumulation (henceforth termed 'available accommodation space') continued to expand as the sea rose over the past few millennia (Fig. 1c). In these situations, high rates of RSLR had the combined effect of promoting accumulation of mineral and organic matter and slowing rates of decomposition. That is, because sedimentation is positively correlated with patterns of inundation frequency[18], rapid accumulation of mineral and organic material is an outcome of the effect of RSLR on increasing inundation. Material that accumulates under conditions of RSLR becomes progressively submerged, creating more anoxic conditions that inhibit more rapid aerobic pathways of organic-matter decomposition. A substantial proportion of the world's tidal marsh[19] occurs in locations regarded to be relatively tectonically and isostatically stable, and their capacity to respond to accelerated RSLR has received little attention. For these coastal wetlands, several millennia of sea-level stability (Fig. 1d) provided considerable time for decomposition of organic material; as organic material was progressively stored near the limit of tidal inundation, decomposition increased under comparatively aerobic conditions.

The available accommodation space is a useful framework for considering the response of tidal wetlands to SLR because it integrates the influence of both tide range and position within the tidal frame[20]. We describe the effective accommodation space within tidal coastal wetlands as being bounded by the bedrock basement, highest astronomical tides (HAT) and hydrodynamic conditions that favour vertical accretion or lateral progradation, rather than sediment entrainment (Fig. 1e). As mineral and organic sediments accumulate, the available accommodation space diminishes (that is, a portion of the effective accommodation space is converted from available to realized

[1]School of Earth, Atmospheric and Life Sciences, University of Wollongong, Wollongong, New South Wales, Australia. [2]Department of Environmental Sciences, Macquarie University, Sydney, New South Wales, Australia. [3]Smithsonian Environmental Research Center, Edgewater, MD, USA. [4]Department of Botany, Nelson Mandela University, Port Elizabeth, South Africa. [5]School of Ecology and Environmental Sciences, Yunnan University, Kunming, China. [6]Australian Nuclear Science and Technology Organisation, Sydney, New South Wales, Australia. *e-mail: kerrylee@uow.edu.au

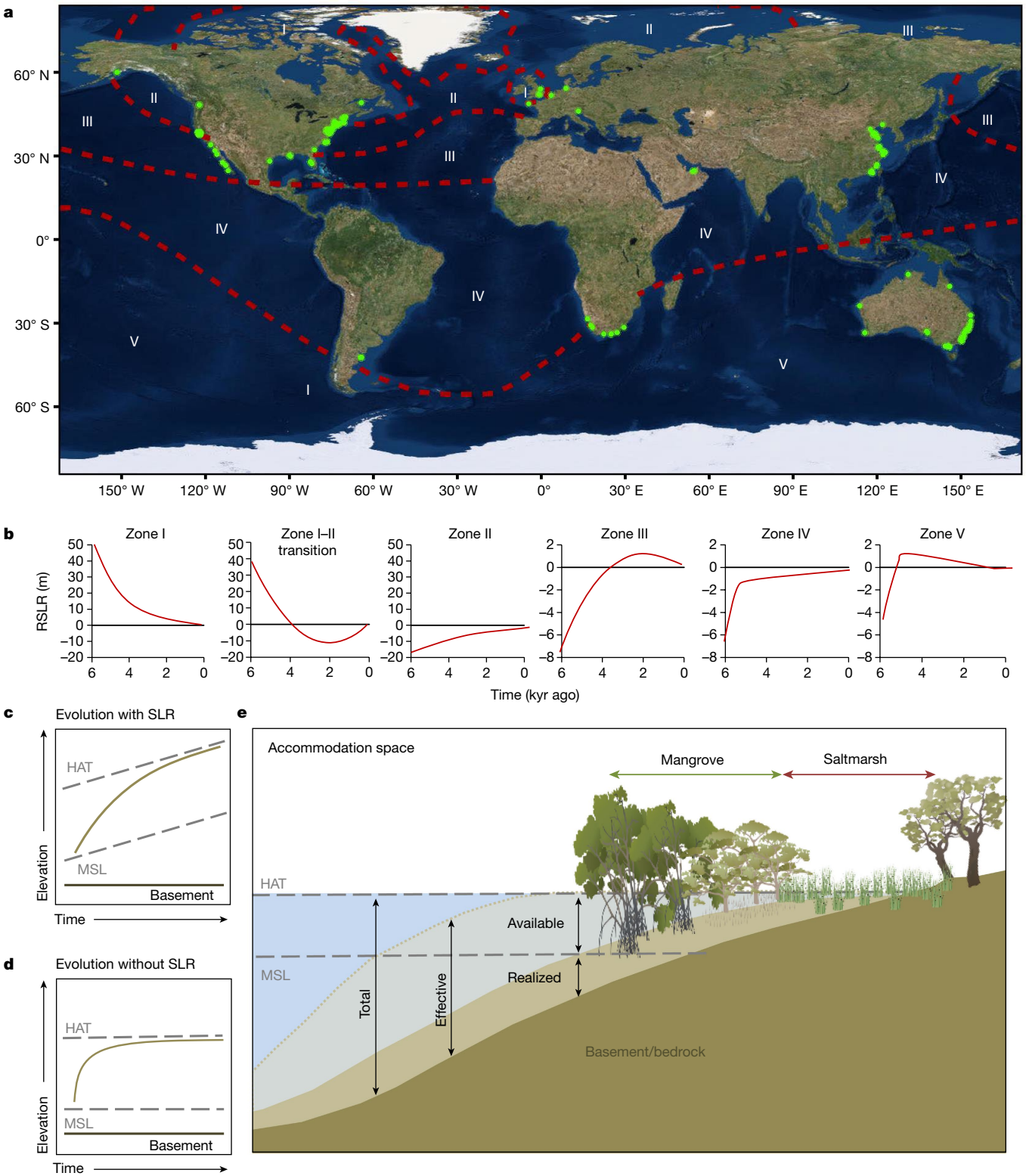

Fig. 1 | Millennial-scale influence of RSL on wetland evolution and accommodation space. a, Holocene RSLR zones and locations of carbon measurements. The figure shows generalized RSLR zones over the Holocene[9] and sample data used in this study, shown as green dots ($n = 345$ locations). Figure adapted with permission from ref. [9], Cambridge Univ. Press; map created with Esri software. **b**, Generalized Holocene relative sea-level history in zones I–V over the past six millennia[9]. Figure adapted with permission from ref. [9], Cambridge Univ. Press. **c**, Wetland surface evolution within an accommodation space defined by the highest astronomical tides (HAT) and mean sea level (MSL), which elevates as the sea rises. **d**, Wetland surface evolution within a stable accommodation space, as occurred in southeastern Australia over the late Holocene[17]. Figures **c** and **d** adapted with permission from ref. [17], Elsevier. **e**, Conceptualized wetland accommodation space, shown here in two dimensions.

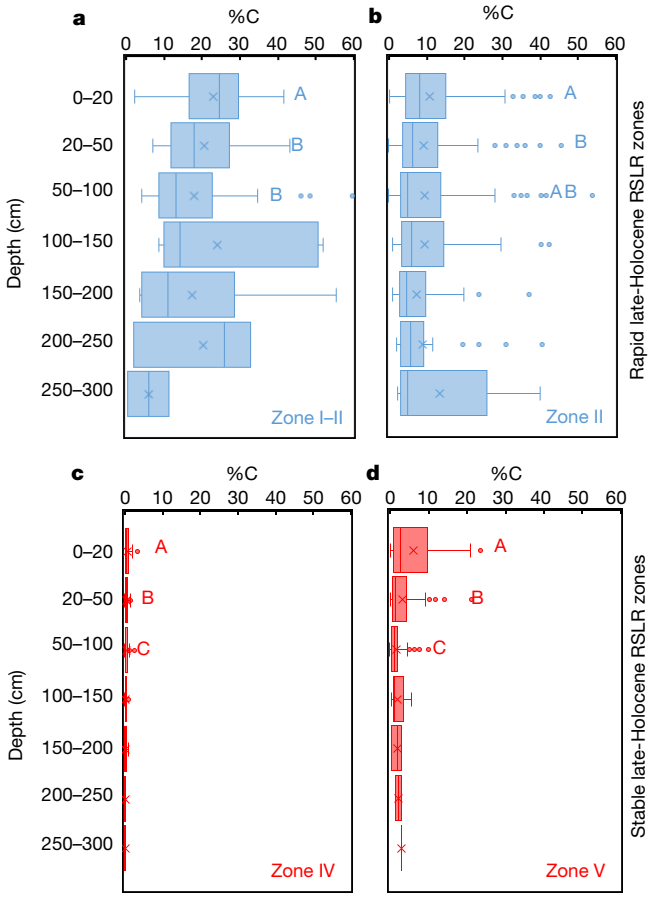

Fig. 2 | Influence of late-Holocene RSLR on carbon concentration. Tidal marshes located along coasts with rapid RSLR in the late Holocene contain higher %C than marshes along coasts with relatively stable sea level. **a**–**d**, Carbon concentration from late-Holocene RSLR over various depths in zone I–II (**a**; rapid RSLR), zone II (**b**; rapid RSLR), zone IV (**c**; stable RSL) and zone V (**d**; stable RSL). Different letters represent significant differences ($P < 0.05$) in %C among depths in the 0–100 cm range within each RSLR zone (that is, depths with the same letter are not significantly different within a zone). Box plots for data-poor RSLR zones (including I and III) are presented in Extended Data Fig. 1.

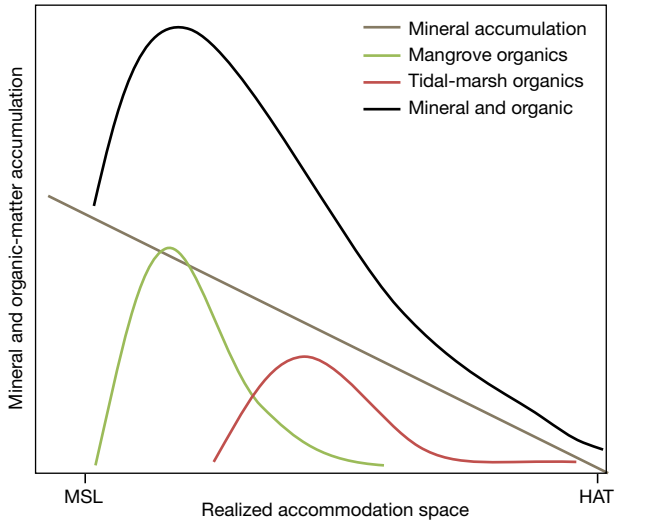

Fig. 3 | Conceptual links between mineral and organic-matter accumulation and realized accommodation space. Model of sediment characteristics with respect to realized accommodation space, here shown in two dimensions to represent the three-dimensional wetland accommodation space. Sedimentation may vary between sites according to mineral and organic sediment availability and to the addition of root material, which is a function of the productivity of vegetation. For simplicity, and following others[30], mineral sediment addition was conceptualized to increase linearly with accommodation space, but may diminish with decreasing accommodation space in an exponential or polynomial manner. Accommodation space varies because of mineral and organic sediment accumulation, SLR and autocompaction. Figure adapted with permission from ref. [30], Springer Nature.

accommodation space; Fig. 1e). This is only alleviated by RSLR, achieved either by subsidence associated with isostatic or tectonic processes, autocompaction of sediments associated with consolidation or decomposition of mineral and organic material, or eustatic SLR, which increases both vertical accommodation space for sediment accumulation and lateral accommodation space for landward encroachment[6]. Addition of bulk organic material from roots further acts to decrease the volume of available accommodation space[21,22].

The coastline of southeastern Australia is an ideal location to explore alterations to wetland accommodation space and SLR because the region is regarded to be relatively tectonically stable[23,24]. Geochronological analyses from a range of biological markers indicate that present sea level was attained approximately 7.8 thousand years (kyr) ago and continued to rise up to 1.5 m above present levels approximately 7.5 kyr ago, falling again to present levels approximately 2 kyr ago[23]. The relative sea-level stability over the past 2 kyr creates favourable conditions to decrease accommodation space and for progradation via accumulation of sediments, provided that sediment is available for deposition (that is, as in Fig. 1d, where elevations evolve without SLR).

Wetlands in this region range from primarily mineral-dominated tidal marshes at elevations high in the tidal frame near HAT to shoreline-fringing mangroves that are relatively lower in the tidal frame. Elevation of the wetland surface in the tidal frame is the relevant variable that indicates accommodation space. As such, low-elevation mangroves at this site are functionally equivalent to low-elevation tidal marshes in climatic regimes that do not support mangroves. Accordingly, mangroves, like lower tidal marsh elsewhere, have more available accommodation space than the adjacent tidal marsh (that is, as per Fig. 1e). In situ vegetation (mangrove and tidal-marsh species within this region) differentially modulates organic-matter additions with deeper root systems of mangrove that are able to add living biomass and organic matter to greater depths within substrates[25], but additions remain proportional to the available accommodation space, as conceptualized in Fig. 3. Under stable sea levels, we might expect organic-matter additions to decline as mineral sediment continues to be delivered by tides and is deposited on wetland surfaces, and the wetland surface approaches the upper limit of the available accommodation space, which is represented by HAT under most conditions, because periodic salt stress prevents encroachment of terrestrial vegetation. Increases in the contribution of organic material lower in the tidal frame would continue as long as accommodation space is available. Accordingly, as SLR increases the available accommodation space, we might expect to see an increase in both mineral additions and carbon storage through burial near wetland surfaces.

To test the effect of RSLR on the available accommodation space and soil organic-carbon accumulation in a zone V wetland, we selected a study site that experienced recent rapid RSLR following subsidence caused by the removal of pillars in an underlying coal mine (Chain Valley Bay, Lake Macquarie, Australia; 33° 10′ S, 151° 35′ E; Supplementary Information). Subsidence corresponded to high-end IPCC projections of SLR in 2100 (about 1 m) but occurred in the space of a few months in 1986. Following subsidence, tidal marsh and adjoining terrestrial vegetation rapidly transitioned to mangrove, and mangrove transitioned to subtidal wetland, over a 5–10 year period. We determined sediment chronologies from cores extracted from substrates that are currently mangrove and submerged.

Vertical accretion in both the mangrove and the submerged wetland increased following RSLR, with high proportional contribution

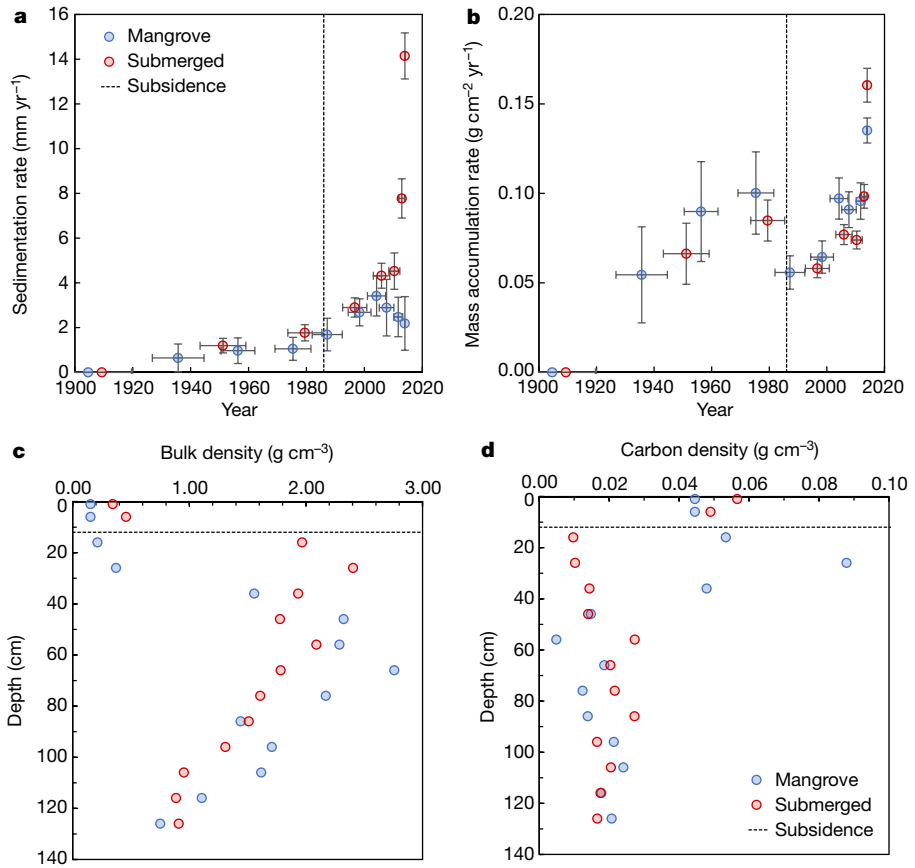

Fig. 4 | Sediment accumulation and character related to available accommodation space. a, **b**, Calculated sedimentation rate (**a**) and mass accumulation rate (**b**) derived from ^{210}Pb dating. Error bars show standard error. **c**, **d**, Bulk density (**c**) and carbon density (**d**) of mangrove (previously tidal marsh and terrestrial vegetation) and submerged (previously mangrove) sediments from Chain Valley Bay (outliers represent modern live root material at that depth). The depth and associated age of sediments at which the subsidence event is evident are indicated by dashed lines. ^{210}Pb activity for mangrove and submerged cores and ^{137}Cs validation of ^{210}Pb chronology are provided in Extended Data Fig. 2.

of carbon-dense organic matter in both settings (Fig. 4). Bulk density rapidly declined following RSLR despite the higher sediment accumulation rate. Sediment accumulation in the new mangrove post-subsidence was approximately double the pre-subsidence rate in the tidal marsh and mangrove, whereas organic-carbon accumulation increased by a factor of four. The sediment and organic-carbon accumulation rate within the newly created subtidal wetland, now a seagrass bed, was still accelerating 30 years after the subsidence event.

We argue that under relatively stable or slightly falling sea levels, as occurred in much of the Southern Hemisphere over the past few millennia, wetlands become increasingly mineral-dominated and favour carbon loss over accumulation as accommodation space diminishes. Our global analysis demonstrates the latent capacity of high organic-carbon accumulation contributing towards elevation gains under conditions in which the available accommodation space increases, as occurs under accelerated RSLR.

These results substantiate that carbon accumulation and storage is related to available accommodation space, which is influenced by rates of RSLR. They imply that SLR will lead to increases in carbon sequestration and storage in many places where vertical accommodation space has previously been constrained by stable or declining sea levels, including southern Africa, Australia, China and South America, which contain half of the global tidal marsh extent[19]. This feedback will be further enhanced where lateral expansion of wetlands in response to RSLR can occur, unless interrupted by storms or other perturbations. A doubling of carbon sequestration rates across wetlands along these coasts could potentially sequester an additional[19] 5 Tg C yr^{-1}, which might provide an important mitigating negative feedback on atmospheric carbon. Wetland loss to clearance[26,27] and impediments to tidal exchange continue to threaten the capacity of coastal wetlands to mitigate climate change[28] both now and in the future as seas continue to rise[29]. Reversing these trends will further improve the carbon sequestration value of coastal wetlands under future, more rapid SLR.

Online content

Any methods, additional references, Nature Research reporting summaries, source data, statements of data availability and associated accession codes are available at https://doi.org/10.1038/s41586-019-0951-7.

Received: 19 December 2017; Accepted: 7 January 2019;
Published online 6 March 2019.

1. Donato, D. C. et al. Mangroves among the most carbon-rich forests in the tropics. *Nat. Geosci.* **4**, 293–297 (2011).
2. Mcleod, E. et al. A blueprint for blue carbon: toward an improved understanding of the role of vegetated coastal habitats in sequestering CO_2. *Front. Ecol. Environ.* **9**, 552–560 (2011).
3. Duarte, C. M., Middelburg, J. & Caraco, N. Major role of marine vegetation on the oceanic carbon cycle. *Biogeosciences* **2**, 1–8 (2005).
4. Kirwan, M. L. & Mudd, S. M. Response of salt-marsh carbon accumulation to climate change. *Nature* **489**, 550–553 (2012).
5. DeLaune, R. & White, J. Will coastal wetlands continue to sequester carbon in response to an increase in global sea level? A case study of the rapidly subsiding Mississippi river deltaic plain. *Clim. Change* **110**, 297–314 (2012).
6. Schuerch, M. et al. Future response of global coastal wetlands to sea-level rise. *Nature* **561**, 231–234 (2018).
7. Holmquist, J. R. et al. Accuracy and precision of tidal wetland soil carbon mapping in the conterminous United States. *Sci. Rep.* **8**, 9478 (2018); corrigendum **8**, 15219 (2018).
8. Murray-Wallace, C. V. & Woodroffe, C. D. *Quaternary Sea-Level Changes: A Global Perspective* (Cambridge Univ. Press, Cambridge, 2014).
9. Clark, J. A., Farrell, W. E. & Peltier, W. R. Global changes in postglacial sea level: a numerical calculation. *Quat. Res.* **9**, 265–287 (1978).
10. Redfield, A. C. Development of a New England salt marsh. *Ecol. Monogr.* **42**, 201–237 (1972).

11. Morris, J. T., Sundareshwar, P. V., Nietch, C. T., Kjerfve, B. & Cahoon, D. R. Responses of coastal wetlands to rising sea-levels. *Ecology* **83**, 2869–2877 (2002).
12. Lovelock, C. E. et al. The vulnerability of Indo-Pacific mangrove forests to sea-level rise. *Nature* **526**, 559–563 (2015).
13. Adam, P. *Saltmarsh Ecology* (Cambridge Univ. Press, Cambridge, 1990).
14. Hiraishi, T. et al. (eds) *2013 Supplement to the 2006 IPCC Guidelines for National Greenhouse Gas Inventories: Wetlands. Technical Report* (IPCC, 2014).
15. Saintilan, N. & Hashimoto, T. R. Mangrove-saltmarsh dynamics on a bay-head delta in the Hawkesbury River estuary, New South Wales, Australia. *Hydrobiologia* **413**, 95–102 (1999).
16. Woodroffe, C. D., Thom, B. G. & Chappell, J. Development of widespread mangrove swamps in mid-Holocene times in northern Australia. *Nature* **317**, 711–713 (1985).
17. Allen, J. R. L. Morphodynamics of Holocene salt marshes: a review sketch from the Atlantic and Southern North Sea coasts of Europe. *Quat. Sci. Rev.* **19**, 1155–1231 (2000).
18. Pethick, J. S. Long-term accretion rates on tidal salt marshes. *J. Sediment. Res.* **51**, 571–577 (1981).
19. Ouyang, X. & Lee, S. Updated estimates of carbon accumulation rates in coastal marsh sediments. *Biogeosciences* **11**, 5057–5071 (2014).
20. Kirwan, M. L. & Guntenspergen, G. R. Influence of tidal range on the stability of coastal marshland. *J. Geophys. Res.* **115**, F02009 (2010).
21. Krauss, K. W. et al. How mangrove forests adjust to rising sea level. *New Phytol.* **202**, 19–34 (2014).
22. Langley, J. A., McKee, K. L., Cahoon, D. R., Cherry, J. A. & Megonigal, J. P. Elevated CO_2 stimulates marsh elevation gain, counterbalancing sea-level rise. *Proc. Natl Acad. Sci. USA* **106**, 6182–6186 (2009).
23. Sloss, C. R., Murray-Wallace, C. V. & Jones, B. G. Holocene sea-level change on the southeast coast of Australia: a review. *Holocene* **17**, 999–1014 (2007).
24. Lambeck, K. & Nakada, M. Late Pleistocene and Holocene sea-level change along the Australian coast. *Palaeogeogr. Palaeoclimatol. Palaeoecol.* **89**, 143–176 (1990).
25. Kelleway, J. J. et al. Seventy years of continuous encroachment substantially increases 'blue carbon' capacity as mangroves replace intertidal salt marshes. *Glob. Change Biol.* **22**, 1097–1109 (2016).
26. Duke, N. C. et al. A world without mangroves? *Science* **317**, 41–42 (2007).
27. Duarte, C., Dennison, W., Orth, R. & Carruthers, T. The charisma of coastal ecosystems: addressing the imbalance. *Estuaries Coasts* **31**, 233–238 (2008).
28. Crooks, S., Herr, D., Tamelander, J., Laffoley, D. & Vandever, J. *Mitigating Climate Change through Restoration and Management of Coastal Wetlands and Near-Shore Marine Ecosystems: Challenges and Opportunities* (World Bank Environment Department, Washington DC, 2011).
29. Pontee, N. Defining coastal squeeze: a discussion. *Ocean Coast. Manage.* **84**, 204–207 (2013).
30. Kirwan, M. L. & Megonigal, J. P. Tidal wetland stability in the face of human impacts and sea-level rise. *Nature* **504**, 53–60 (2013).

Acknowledgements This research was supported by the Australian Research Council (FT130100532), AINSE (ALNGRA13046) and the UOW Global Challenges Program. The Smithsonian Environmental Research Center supported J.P.M., J.R.H, M.L. and L.S.-B. The data curation efforts of J.R.H. and data collection and synthesis efforts of J.P.M. were supported by United States National Science Foundation grants to the Coastal Carbon Research Coordination Network (DEB-1655622) and the Global Change Research Wetland (DEB-0950080, DEB-1457100 and DEB-1557009) and by a NASA Carbon Monitoring System programme grant (NNH14AY67I). L.S.-B. was supported by a Smithsonian Institution MarineGEO Postdoctoral Fellowship. This is contribution number 32 of the Smithsonian's MarineGEO Network. The authors acknowledge J. Curran for assistance with sample preparation, S. Rasel, S. Oyston and M. Rupic for assistance with data collation and the students who undertook fieldwork as part of this research.

Reviewer information *Nature* thanks Andrew Ashton and the other anonymous reviewer(s) for their contribution to the peer review of this work.

Author contributions K.R., N.S. and C.D.W. developed the premise of the study. J.J.K., N.S., J.P.M., J.B.A., J.R.H., M.L., L.S.-B. and K.R. gathered and produced input data for the global analysis. J.J.K. carried out global-scale statistical analyses. K.R., D.M. and A.Z. undertook local-study fieldwork, sample preparation, laboratory and statistical analyses. K.R., J.J.K., N.S. and C.D.W. wrote the paper. All authors contributed to editing and revising the paper.

Competing interests The authors declare no competing interests.

Additional information
Extended data is available for this paper at https://doi.org/10.1038/s41586-019-0951-7.
Supplementary information is available for this paper at https://doi.org/10.1038/s41586-019-0951-7.
Reprints and permissions information is available at http://www.nature.com/reprints.
Correspondence and requests for materials should be addressed to K.R.
Publisher's note: Springer Nature remains neutral with regard to jurisdictional claims in published maps and institutional affiliations.

METHODS

Review of global tidal marsh carbon accumulation. Tidal marshes were the focus of our global analysis owing to their global distribution relative to other tidal wetlands (that is, mangroves). We collated published records of carbon concentration or organic matter concentration in tidal marshes because these are the two most widely reported measures related to carbon content and are less confounded by variation in mineral content and methodological error than values that incorporate bulk density (for example, grams of carbon per cubic centimetre or grams of organic matter per cubic centimetre). We tested the sensitivity of our results to the choice of carbon content and bulk density and confirmed that these two metrics produce similar patterns with respect to the role of RSLR variation on C sequestration (Supplementary Information, Extended Data Fig. 4, Extended Data Tables 4–6). This collation of records included research theses, national data collations, unpublished data and studies identified by previous reviews[19,31] and incorporated new literature identified using the same search terms as Ouyang and Lee[19] (Supplementary Information). We then identified records that contained data across the active root zone (0–20 cm), medium-depth (20–50 cm) and deeper (50–100 cm) depth intervals and beyond. This was undertaken to (i) compare the influence of the active root zone among RSLR zones and (ii) assess carbon accumulation across a period of centuries to millennia on the basis of global rates of tidal marsh accumulation[19] of <10 mm yr^{-1}. Organic-matter concentration data were converted[32] to %C. When multiple cores were available for a study location, we calculated mean %C values across replicate cores for each depth interval. Study locations with different geomorphic or floristic characteristics within a marsh were deemed to be different study locations for this purpose. The vast majority of studies retained live and dead roots in their analysis, although there were regional exceptions to this. For example, all Chinese records (zone IV) removed roots before %C analysis. To account for potential confounding effects of zones and methods, we recorded the aperture of the sieve and included it as a covariate in statistical analyses.

This approach resulted in a database comprising 1,266 depth-interval records across 345 locations (Supplementary Information). Data were assigned to RSLR zones on the basis of local or regional Holocene sea-level curves[24,33,34]. A linear mixed model[35] was used to assess the relationships between the dependent variable soil %C and the fixed factors of soil depth (three repeated measure levels: 0–20 cm, 20–50 cm and 50–100 cm) and RSLR zone (eight levels: zones I through V and transitional regions I–II, II–III and IV–V). The influence of climate and salinity was also tested using a linear mixed model (Supplementary Information). Climate was found to be insignificant (Extended Data Table 1a), whereas extremely weak linear-regression relationships between salinity and %C were identified over three depth intervals ($R^2 < 0.07$, $P < 0.001$; Extended Data Fig. 3), with little effect on the significance of RSLR zone on %C in the linear mixed model (Extended Data Table 1b).

To further assess variations in %C with soil depth, a separate repeated-measures analysis of variance (RM-ANOVA)[36] was completed for each RSLR zone. RM-ANOVA is a test to identify significant differences within related groups, in this case identifying differences in %C with soil depth down a core. Linear mixed-model pairwise comparisons and RM-ANOVA outcomes are reported for the data-rich RSLR zones II (156 locations), IV (68 locations), V (63 locations) and I–II transition (36 locations). Other RSLR zones (I and III) and transitional regions were considered data-poor and were excluded from these pairwise comparisons.

Core extraction and sediment characterization. Continuous cores of approximately 1.5–2 m length were extracted within vegetation zones along two transects that were normal to the vegetation zonation and the shoreline of Chain Valley Bay, Lake Macquarie (see detailed site description in the Supplementary Information). The sediment character of all cores was determined. Detailed analysis of bulk density, grain size and carbon and nitrogen content, as well as carbon and nitrogen stable-isotope analysis, were undertaken on selected cores. This paper presents information on the submerged wetland and mangrove core. Grainsize analysis was undertaken using a Malvern Mastersizer 2000 laser diffractometer. Elemental analysis and stable isotope analysis was undertaken using a continuous-flow isotope-ratio mass spectrometer (Delta V Plus, Thermo Scientific) interfaced with an elemental analyser (Thermo Fisher Flash 2000 HT EA, Thermo Electron).

Radiometric sediment dating. Sediment samples from cores that underwent detailed sediment characterization were also processed for ^{210}Pb and ^{137}Cs radiometric dating to determine rates of sediment accumulation. Sediment cores were sliced at 1-cm intervals and prepared for analysis of excess ^{210}Pb activities using α-particle spectrometry[37]. Bulk samples were prepared for ^{137}Cs activity analysis using γ-ray spectrometry. All analyses were undertaken at the Australian Nuclear Science and Technology Organisation (ANSTO). Recent sediment chronologies derived from analysis of excess ^{210}Pb activities were determined using the Constant Rate of Supply (CRS) model and validated using the presence of a subsurface peak in the ^{137}Cs activity concentration for each core, which marks the 1963 depth[38].

Data availability

The data used in the global analysis of carbon concentration with respect to Holocene RSLR are provided in the Supplementary Information. The data that support the Chain Valley Bay study site analysis are available from the corresponding author upon reasonable request.

31. Chmura, G. L., Anisfeld, S. C., Cahoon, D. R. & Lynch, J. C. Global carbon sequestration in tidal, saline wetland soils. *Glob. Biogeochem. Cycles* **17**, 1111 (2003).
32. Craft, C., Seneca, E. & Broome, S. Loss on ignition and Kjeldahl digestion for estimating organic carbon and total nitrogen in estuarine marsh soils: calibration with dry combustion. *Estuaries Coasts* **14**, 175–179 (1991).
33. Shennan, I. & Horton, B. Holocene land- and sea-level changes in Great Britain. *J. Quaternary Sci.* **17**, 511–526 (2002).
34. Pluet, J. & Pirazzoli, P. *World Atlas of Holocene Sea-Level Changes* Vol. 58 (Elsevier, Amsterdam, 1991).
35. Verbeke, G. in *Linear Mixed Models in Practice* (eds Verbeke, G. & Molenberghs, G.) 63–153 (Springer, New York, 1997).
36. von Ende, C. N. in *Design and Analysis of Ecological Experiments* (eds Scheiner, S. M. & Gurevitch, J.) 134–157 (Oxford Univ. Press, New York, 2001).
37. Hollins, S. et al. Reconstructing recent sedimentation in two urbanised coastal lagoons (NSW, Australia) using radioisotopes and geochemistry. *J. Paleolimnol.* **46**, 579–596 (2011).
38. Appleby, P. in *Tracking Environmental Change Using Lake Sediments* (eds Smol, J. P. et al.) 171–203 (Kluwer, Dordrecht 2001).

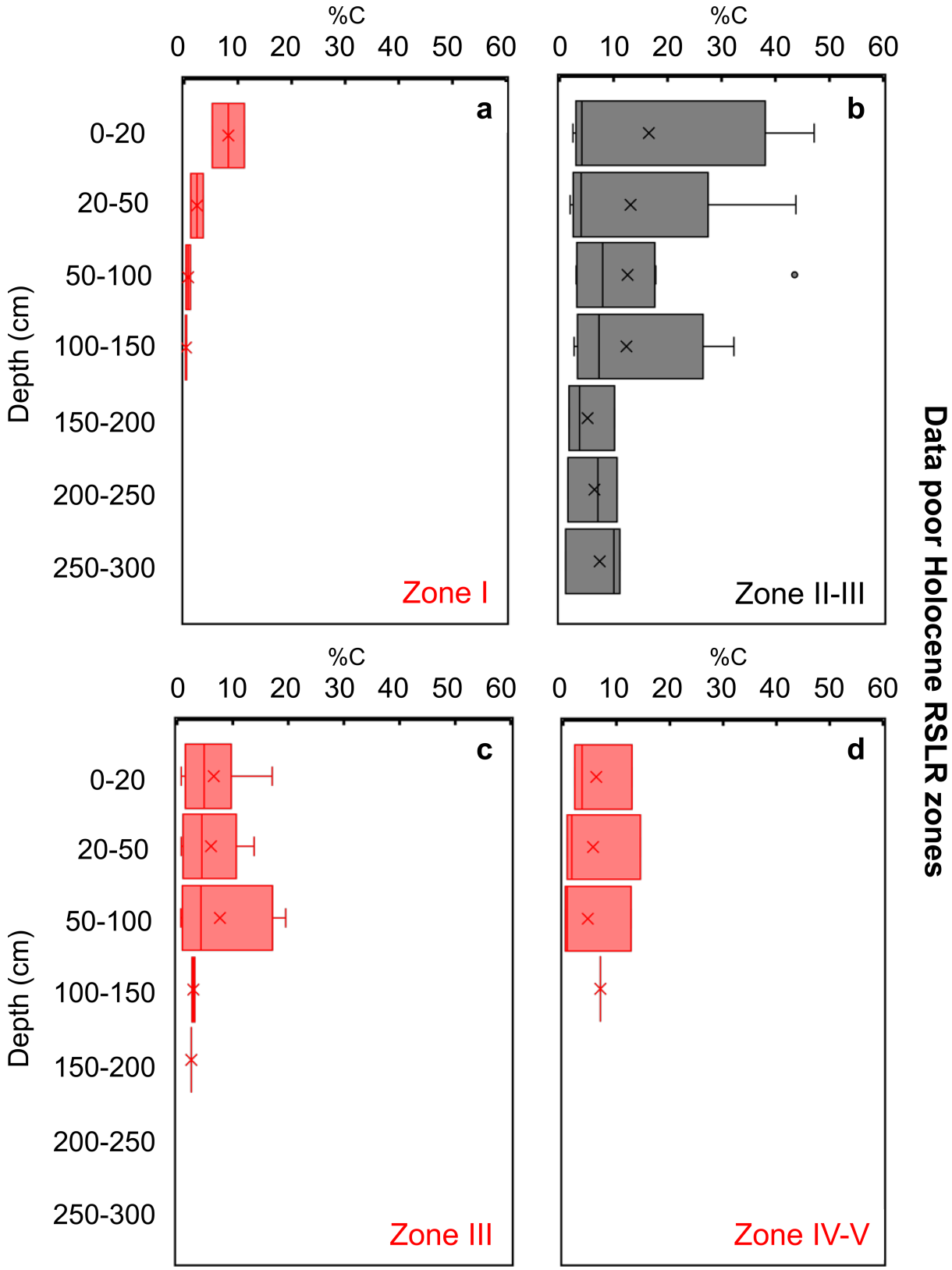

Extended Data Fig. 1 | Relationship between late-Holocene RSLR and carbon concentration for data-poor late-Holocene RSLR zones and transitional zones. a–d, Box plots of tidal-marsh soil C concentration for data-poor Holocene RSLR zones and transitional regions: zone I (**a**), zone II–III transition (**b**), zone III (**c**) and zone IV–V transition (**d**).

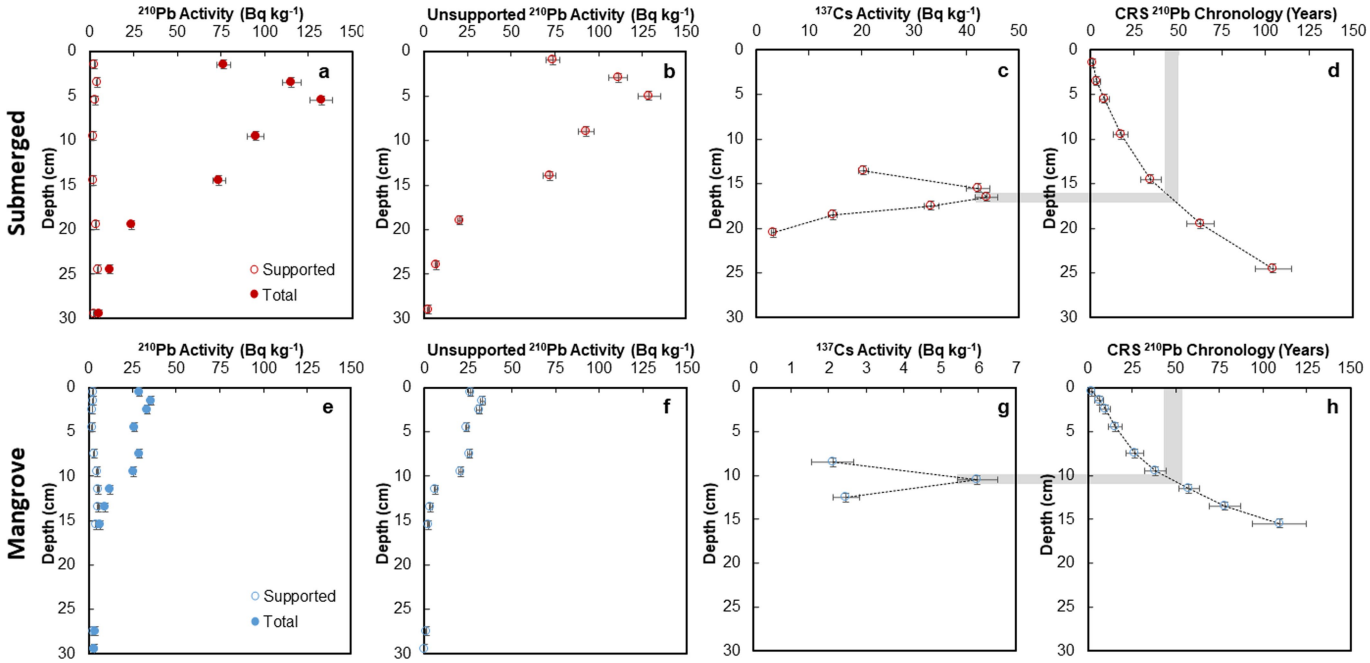

Extended Data Fig. 2 | ^{210}Pb and ^{137}Cs activity of submerged and mangrove sediments. a–d, Submerged-core supported and total (**a**) and unsupported (**b**) ^{210}Pb activity, ^{137}Cs activity (**c**) and CRS-based ^{210}Pb chronology (**d**). **e–h**, Mangrove-core supported and total (**e**) and unsupported (**f**) ^{210}Pb activity, ^{137}Cs activity (**g**) and CRS-based ^{210}Pb chronology (**h**). The grey validation lines confirm that the ^{137}Cs activity peak corresponds to a sediment date of 1963, in agreement with CRS-based ^{210}Pb chronology (core dating occurred in 2014).

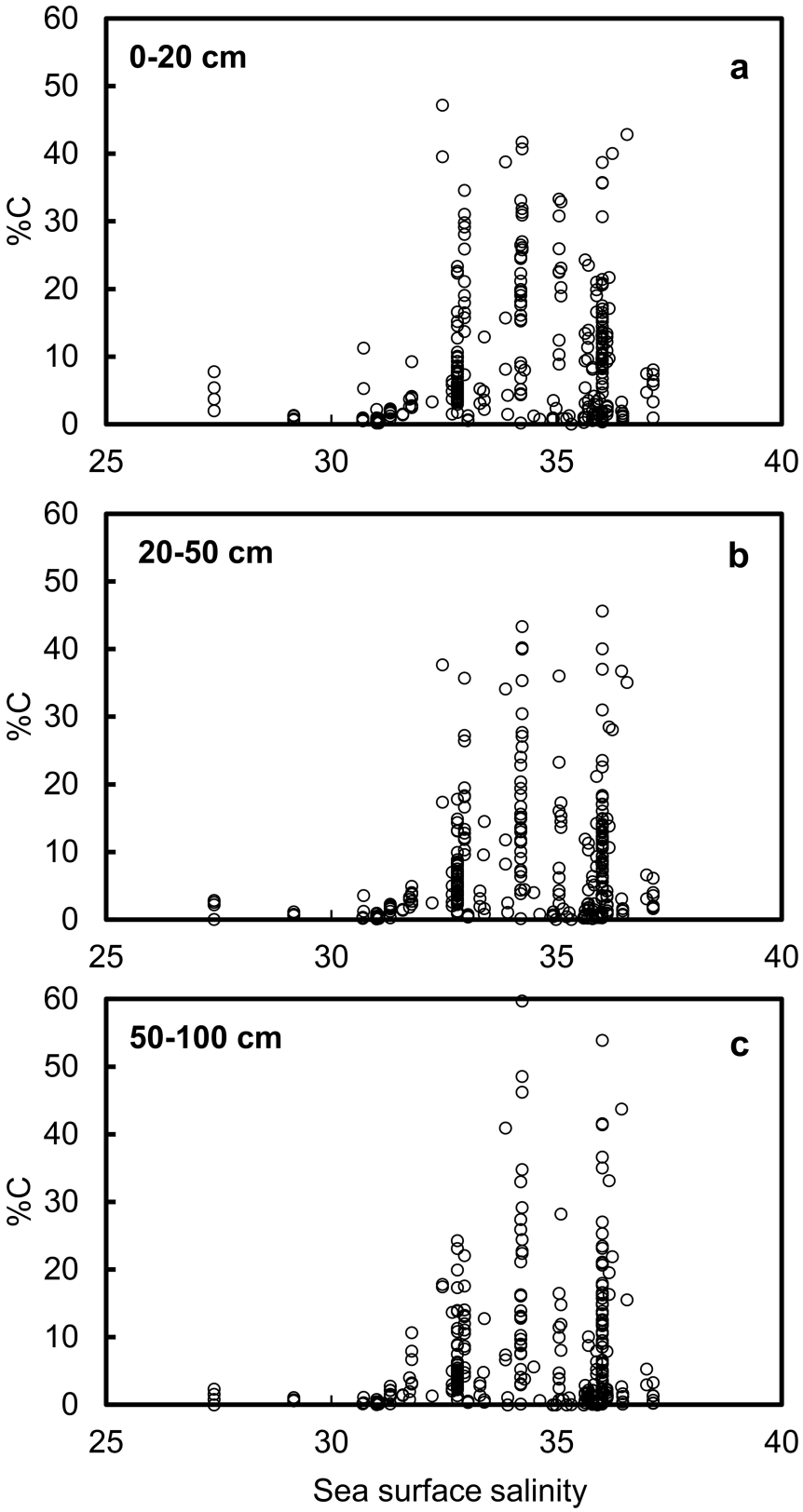

Extended Data Fig. 3 | Relationship between sea-surface salinity and C concentration over three depth intervals. a–c, Regression analysis of C concentration and global-scale sea-surface salinity, derived from the NASA Aquarius Satellite Mission, exhibited extremely weak relationships over the depth intervals 0–20 cm (**a**; $R^2 = 0.07$, $P < 0.001$), 20–50 cm (**b**; $R^2 = 0.07$, $P < 0.01$) and 50–100 cm (**c**; $R^2 = 0.06$, $P < 0.001$). Soil %C values are low for zones I and IV in part owing to the removal of roots before analysis (see Supplementary Table 1).

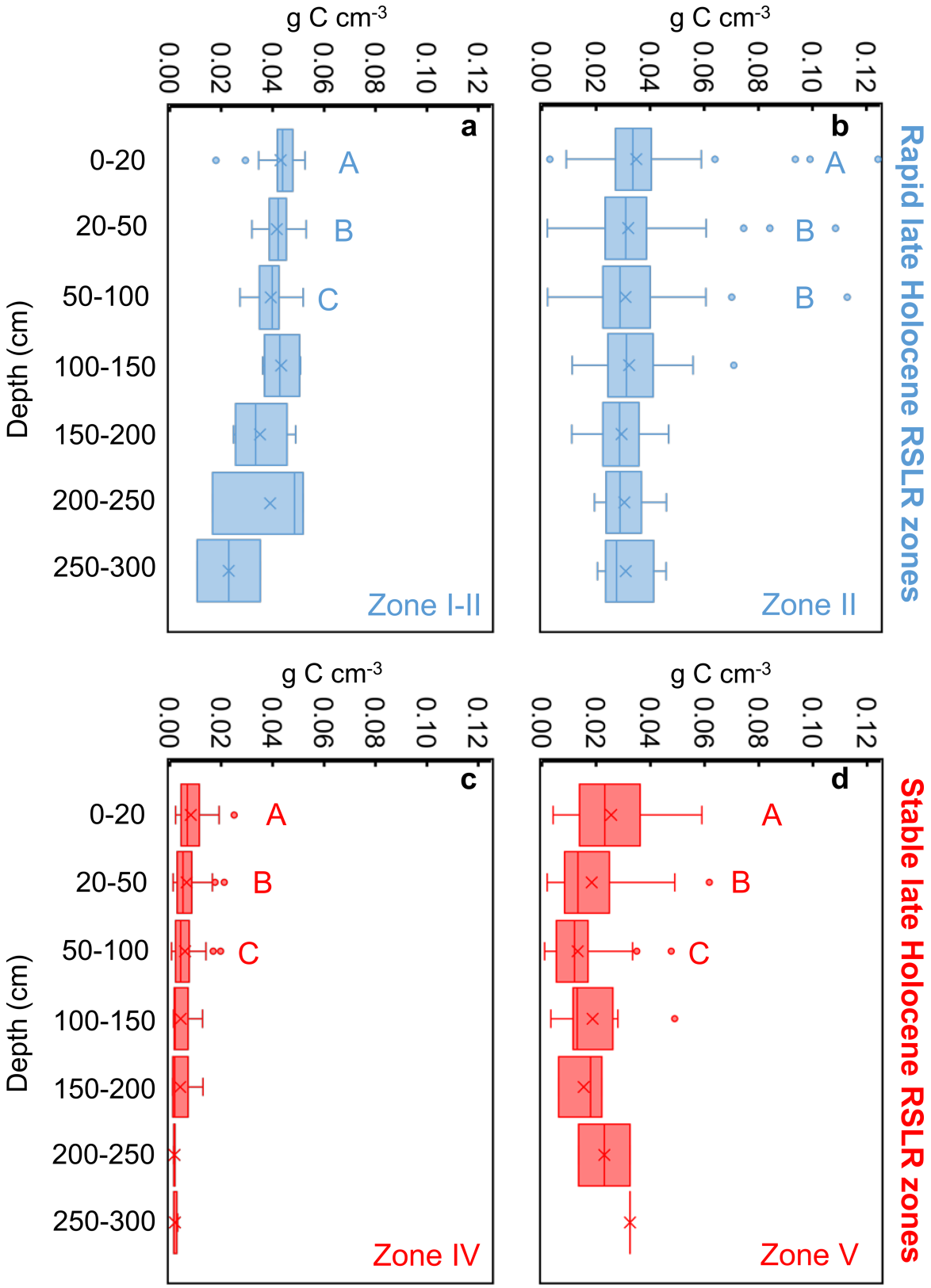

Extended Data Fig. 4 | Relationship between late-Holocene RSLR and C density for data-rich late-Holocene RSLR zones and transitional zones. **a–d**, Box plots of tidal-marsh soil C density for data-rich Holocene RSLR zones and transitional regions: zone I–II transition (**a**), zone II (**b**), zone IV (**c**), and zone V (**d**).

Extended Data Table 1 | Results of the linear mixed model used for the dependent variable of tidal-marsh soil carbon concentration

a) Model with sieve size as a random factor covariate

Source	Numerator df	Denominator df	F-value	P-value
Intercept	1	328.9	28.134	**<0.001**
Soil Depth	2	330.5	3.922	**0.021**
RSLR Zone	6	297.2	31.464	**<0.001**
Köppen Climate Zone	2	326.4	1.657	0.192
Depth * RSLR Zone	14	333.0	1.847	**0.031**

b) Model with salinity as a random factor covariate

Source	Numerator df	Denominator df	F-value	P-value
Intercept	1	252.4	19.868	**<0.001**
Soil Depth	2	335.0	4.171	**0.016**
RSLR Zone	6	332.246	34.931	**<0.001**
Köppen Climate Zone	2	332.271	0.466	0.628
Depth * RSLR Zone	14	335.0	1.878	**0.028**

Analysis was restricted to the three soil depths for which %C data were most commonly available (0–20 cm, 20–50 cm and 50–100 cm). **a**, The sieve size was included in the model as a random factor covariate. **b**, The salinity was included in the model as a random factor covariate. 'Numerator df' refers to the degrees of freedom (df) of the regression; 'denominator df' refers to the degrees of freedom of the residuals; 'F-value' refers to the ratio of between-group variability to within-group variability.

Extended Data Table 2 | Results of linear-mixed-model pairwise comparisons among Holocene RSLR zones for the dependent variable of tidal-marsh soil carbon concentration

		RAPID HOLOCENE RSLR ZONES		STABLE HOLOCENE RSLR ZONES		
	RSLR zone	I-II transition (36)	II (156)	IV (68)	V (63)	
RAPID HOLOCENE RSLR ZONES	I-II transition (36)		**I-II > II**	**I-II > IV**	**I-II > V**	**COMPARISON DIRECTION**
	II (156)	**<0.001**		**II > IV**	**II > V**	
STABLE HOLOCENE RSLR ZONES	IV (68)	**<0.001**	**<0.001**		IV ≈ V	
	V (63)	**<0.001**	**<0.001**	1.0		
		P-VALUES				

The top right of the table shows the direction of pairwise comparisons and the bottom left of the table shows the corresponding *P* values, obtained using estimated marginal means with the Bonferroni adjustment. Pairwise comparisons that are significantly different at $P < 0.05$ are in bold. Values in parentheses indicate the number of soil cores included in the analysis from each sea-level zone.

Extended Data Table 3 | Results of global data compilation of tidal marsh soil carbon concentration and RM-ANOVA

Late-Holocene RSLR zone	Number of locations	%C by depth interval			RM-ANOVA		
		0-20cm	20-50cm	50-100cm	df	*F*-value	*P*-value
Rapid RSLR zones:							
I-II transition	36	23.6 ± 1.5^{A}	20.6 ± 1.7^{B}	18.1 ± 2.2^{B}	1.8, 60	7.771	**0.002**
II	156	10.9 ± 0.7^{A}	9.3 ± 0.7^{B}	9.5 ± 0.8^{AB}	1.5, 236	5.847	**0.007**
Stable RSLR zones:							
IV*	68	0.78 ± 0.07^{A}	0.62 ± 0.06^{B}	0.56 ± 0.07^{C}	1.4, 89	26.127	**<0.001**
V	63	6.8 ± 0.9^{A}	3.4 ± 0.6^{B}	2.0 ± 0.3^{C}	1.4, 77	32.311	**<0.001**
Data Poor zones:							
I*	2	8.2 ± 3.0	2.4 ± 1.2	0.7 ± 0.4		N/A	
II-III transition	9	16.6 ± 6.2	13.1 ± 5.5	12.6 ± 4.3		N/A	
III	7	4.5 ± 1.2	4.2 ± 1.4	3.1 ± 0.8		N/A	
IV-V transition	3	6.2 ± 3.4	5.6 ± 4.4	4.6 ± 4.1		N/A	

Values reported are the number of distinct study locations for which relevant data were available, as well as mean soil %C (± one standard error) for the most commonly reported depth intervals: 0–20 cm, 20–50 cm and 50–100 cm. A separate RM-ANOVA was conducted for each data-rich Holocene RSL zone to test for differences in tidal-marsh soil %C values among soil depth intervals. *P* values are based on estimated marginal means with the Bonferroni adjustment, with values significant at $P < 0.05$ in bold. Superscript letters denote significantly different depth intervals within each SLR zone.

Extended Data Table 4 | Results of the linear mixed model for the dependent variable of tidal marsh soil carbon density (in grams of carbon per cubic centimetre)

a) Model with sieve size as a random factor covariate

Source	Numerator df	Denominator df	F-value	P-value
Intercept	1	331.629	192.586	**<0.001**
Soil Depth	2	331.076	17.552	**<0.001**
RSLR Zone	6	333.036	62.070	**<0.001**
Köppen Climate Zone	2	332.151	1.084	0.339
Depth * RSLR Zone	14	348.530	3.822	**<0.001**

b) Model with salinity as a random factor covariate

Source	Numerator df	Denominator df	F-value	P-value
Intercept	1	285.765	14.538	**<0.001**
Soil Depth	2	330.326	17.553	**<0.001**
RSLR Zone	6	331.574	55.270	**<0.001**
Köppen Climate Zone	2	330.375	1.349	0.261
Depth * RSLR Zone	14	346.841	3.792	**<0.001**

Analysis was restricted to three soil depths: 0–20 cm, 20–50 cm and 50–100 cm. **a**, The sieve size (in millimetres) was included in the model as a random factor covariate. **b**, The salinity was included in the model as a random factor covariate.

Extended Data Table 5 | Results of linear-mixed-model pairwise comparisons among Holocene RSLR zones for the dependent variable of tidal-marsh soil carbon density (in grams of carbon per cubic centimetre)

		RAPID HOLOCENE RSLR ZONES		STABLE HOLOCENE RSLR ZONES		
	RSLR zone	I-II transition (36)	II (156)	IV (68)	V (63)	
RAPID HOLOCENE RSLR ZONES	I-II transition (36)		**I-II > II**	**I-II > IV**	**I-II > V**	**COMPARISON DIRECTION**
	II (156)	**0.006**		**II > IV**	**II > V**	
STABLE HOLOCENE RSLR ZONES	IV (68)	**<0.001**	**<0.001**		**IV < V**	
	V (63)	**<0.001**	**<0.001**	<0.001		
		P-VALUES				

The top right of the table shows the direction of pairwise comparisons and the bottom left of the table shows the corresponding *P* values, obtained using estimated marginal means with the Bonferroni adjustment. Pairwise comparisons that are significantly different at $P < 0.05$ are in bold. Values in parentheses indicate the number of soil cores included in the analysis from each sea-level zone.

Extended Data Table 6 | Results of global data compilation of tidal marsh soil carbon density and RM-ANOVA

Late-Holocene RSLR zone	Number of locations	g C cm^{-3} by depth interval			RM-ANOVA	
		0-20cm	20-50cm	50-100cm	df	*F*-value *P*-value
Rapid RSLR zones:						
I-II transition	36	0.044 ± 0.001 ^{A}	0.042 ± 0.001 ^{B}	0.039 ± 0.001 ^{C}	1.4, 49	13.079 <**0.001**
II	156	0.035 ± 0.001 ^{A}	0.032 ± 0.001 ^{B}	0.031 ± 0.001 ^{B}	1.5, 226	12.895 <**0.001**
Stable RSLR zones:						
IV*	68	0.008 ± 0.001 ^{A}	0.006 ± 0.001 ^{B}	0.006± 0.001 ^{C}	1.5, 95	35.457 <**0.001**
V	63	0.027 ± 0.002 ^{A}	0.018 ± 0.002 ^{B}	0.014 ± 0.001 ^{C}	1.6, 90	33.226 <**0.001**
Data Poor zones:						
I*	2	0.034 ± 0.004	0.020 ± 0.006	0.009 ± 0.004	N/A	
II-III transition	9	0.034 ± 0.005	0.035 ± 0.006	0.034 ± 0.004	N/A	
III	7	0.040 ± 0.013	0.035 ± 0.011	0.031 ± 0.009	N/A	
IV-V transition	3	0.025 ± 0.006	0.020 ± 0.009	0.016 ± 0.010	N/A	

Values reported are the number of distinct study locations for which relevant data were available, as well as the mean soil carbon density (in grams of carbon per cubic centimetre) (± one standard error) for the most commonly reported depth intervals: 0–20 cm, 20–50 cm and 50–100 cm. A separate RM-ANOVA was conducted for each data-rich Holocene RSLR zone to test for differences in tidal-marsh soil carbon density among soil depth intervals. *P* values are based on estimated marginal means with the Bonferroni adjustment, with values significant at $P < 0.05$ in bold. Superscript letters denote significantly different depth intervals within each SLR zone.

*Soil C density values are low for zones I and IV in part owing to the removal of roots before analysis (see Supplementary Table 1).